Frontiers of Optoelectronics (2023) 16:41
https://doi.org/10.1007/s12200-023-00096-x

Frontiers of Optoelectronics

LETTER

Enhancement of silicon sub-bandgap photodetection by helium-ion implantation

Zhao Wang[1,2] · Xiaolei Wen[3] · Kai Zou[1,2] · Yun Meng[1,2] · Jinwei Zeng[4,5] · Jian Wang[4,5] · Huan Hu[6,7] · Xiaolong Hu[1,2,4]

Received: 13 September 2023 / Accepted: 3 November 2023

Abstract

Silicon sub-bandgap photodetectors can detect light at the infrared telecommunication wavelengths but with relatively weak photo-response. In this work, we demonstrate the enhancement of sub-bandgap photodetection in silicon by helium-ion implantation, without affecting the transparency that is an important beneficial feature of this type of photodetectors. With an implantation dose of 1×10^{13} ions/cm^2, the minimal detectable optical power can be improved from -33.2 to -63.1 dBm, or, by 29.9 dB, at the wavelength of 1550 nm, and the photo-response at the same optical power (-10 dBm) can be enhanced by approximately 18.8 dB. Our work provides a method for strategically modifying the intrinsic trade-off between transparency and strong photo-responses of this type of photodetectors.

Keywords Sub-bandgap optical absorption · Helium-ion implantation · Silicon photodetector · Non-invasive photodetection

1 Introduction

Harnessing sub-bandgap optical absorption in semiconductors can extend the photo-response spectra of photodetectors beyond the long-wavelength limit [1–7]. One of the specific applications of sub-bandgap optical absorption is the contactless integrated photonic probe (CLIPPs). These devices were made to non-invasively monitor the changes and fluctuations of optical power in silicon waveguides and on more sophisticated photonic circuits [1], and they were combined with feedback systems for feedback control of photonic integrated circuits [2]. By optimizing the device structure [3] or reducing noise [4], the sensitivity of CLIPPs has been further improved. Additionally, normal-incidence silicon photodetectors that are analogous to CLIPPs and that can detect free-space light at the infrared telecommunication wavelengths have been demonstrated [5, 6]; four-quadrant photodetectors have been designed and made to track the positions and deflections of light beams in free space [7].

One important feature of these photodetectors is their non-invasiveness, or, transparency, and in this respect, they are quite different from commonly used photodetectors. The fundamental reason for this feature is that sub-bandgap optical absorption is weak, compared with inter-band optical absorption. This benefit leads to many applications; however, it also means that these photodetectors show low sensitivity and limited photo-responsivity, which may not work well, or may fail, when the to-be-detected light is faint. Indeed, non-invasiveness, or transparency, and strong photo-response are trade-off behaviors.

This trade-off can be mitigated by defect-state engineering [8, 9]. Strategically increasing the density of defect states within the bandgap by ion implantation can enhance the

✉ Huan Hu
huanhu@intl.zju.edu.cn

✉ Xiaolong Hu
xiaolonghu@tju.edu.cn

1 School of Precision Instrument and Optoelectronic Engineering, Tianjin University, Tianjin 300072, China

2 Key Laboratory of Optoelectronic Information Science and Technology, Ministry of Education, Tianjin 300072, China

3 Center for Micro and Nanoscale Research and Fabrication, University of Science and Technology of China, Hefei 230026, China

4 Wuhan National Laboratory for Optoelectronics, Huazhong University of Science and Technology, Wuhan 430074, China

5 Optics Valley Laboratory, Wuhan 430074, China

6 ZJUI Institute, International Campus, Zhejiang University, Haining 311400, China

7 State Key Laboratory of Fluidic Power & Mechanical Systems, Zhejiang University, Hangzhou 310027, China

Published online: 06 December 2023

photo-response, without noticeably sacrificing the non-invasiveness or transparency. In Ref. [10], researchers implanted helium ions by ion implanter to silicon waveguides to fabricate in-line photodetectors that can work in the wavelength range between 1400 and 1590 nm.

In a broader context, ion implantation has important impact on the performance of photodetectors in general. Researchers have implanted B ions into silicon-based mesa heterojunction photodetectors and found that ion implantation significantly improved the photoelectric properties of devices [11]; other researchers have implanted Zr ions into $CsPbBr_3$ perovskite single-crystal photodetectors to enhance the performances of the devices [12]; others have studied the photoelectrical performance of Schottky photodetectors made of β-Ga_2O_3 implanted with Mg ions [13]; some have implanted Argon ions to silicon Schottky-type photodetectors to enhance the responsivity at infrared 1.31 and 1.55 μm [14]. Additionally, ion implantation has been found to have impact on the nonlinear properties of silicon [15].

In this letter, we report use of a helium-ion microscope to implant helium ions into normal-incidence silicon sub-bandgap photodetectors [5]. The helium-ion microscope offers the capability of implanting with a super small beam spot of ~ 0.5 nm and has demonstrated promising applications in modifying material properties for superconducting junctions [16] and memristors [17]. Here we report the experiment on applying helium-ion beam implantation to enhance the photo-response and sensitivity beyond the long-wavelength limit without affecting the transparency of the sub-bandgap photodetector. Our experimental results show that by implanting helium ions with relatively low dose influences (1×10^{13} ions/cm^2), the minimal detectable optical power can be improved from − 33.2 to − 63.1 dBm at the wavelength of 1550 nm. Moreover, the photo-response at the same optical power (− 10 dBm) can be enhanced by approximately 18.8 dB (with a dose of 1×10^{13} ions/cm^2). The transmittance spectra from 1200 to 1800 nm, with and without helium-ion implantation, stay almost unchanged, confirming that the transparency of the photodetector is not noticeably affected.

2 Experiments

The silicon sub-bandgap photodetector was fabricated on a silicon-on-insulator (SOI) wafer using the same recipe as reported in Ref. [5], with an additional step to strip the residual photoresist on top of the photodetector by immersing the chip in hot *N*-methyl pyrrolidone (NMP) at 95 ℃ for 30 min. The photosensitive area of the photodetector was 5 μm by 5 μm, and the thickness of the top silicon was 220 nm. The optical micrograph of the photodetector is shown in Fig. 1a. The region in the dashed box was 6.5 μm by 6.5 μm and was the region for helium-ion implantation. Figure 1b presents the schematic drawing of helium-ion implantation, using a helium-ion microscope. In the process of implantation, the helium-ion beam scanned over the area in the dashed box with a step size of 0.25 nm. We precisely controlled the dose by precisely controlling the beam current of the helium-ion microscope and writing/implantation time. The helium-ion microscope we used had a beam gating time precision of 0.1 μs, and we used a beam current of 0.5 pA.

We simulated the distribution and density of helium ions and defects generated by ion bombardment, using the software SRIM, which was based on the Monte-Carlo method [18]. Figure 1c and e present the distribution of helium ions and defects per unit dose, respectively, in both the top silicon and silicon oxide layers. The accelerating voltage was 30 kV. Figure 1d and f present N_{He^+} and N_{Def}, as a function of the dose, at three accelerating voltages, 10, 30, and 50 kV. Note that for the same dose, increasing the accelerating voltage decreased both N_{He^+} and N_{Def}. In our experiment, we kept the doses low to avoid material swelling [8] that could affect the optical properties of the photodetectors. We used a 30 kV accelerating voltage and doses of 1×10^{13}, 5×10^{13}, 1×10^{14} and 1×10^{15} ions/cm^2 in the experiment and N_{He^+} values estimated by the simulation were 8.7×10^{16}, 4.4×10^{17}, 8.7×10^{17} and 8.7×10^{18} cm^{-3} for these four doses, respectively, and N_{Def} values were estimated to be 3.1×10^{19}, 1.6×10^{20}, 3.1×10^{20} and 3.1×10^{21} cm^{-3}, respectively.

The experimental setup, as schematically presented in Fig. 1g, and the method to characterize the silicon sub-bandgap photodetectors were almost identical to those reported in Ref. [5]. Very briefly, we used a lensed fiber with a spot mode field diameter of 2 μm for vertical laser illumination of the surface of the photosensitive area of the silicon sub-bandgap photodetector; the optical power to the silicon sub-bandgap photodetector could be adjusted by a variable optical attenuator. The silicon sub-bandgap photodetector was driven by an AC voltage, $V(f)$, from a lock-in amplifier, and the current signal from silicon sub-bandgap photodetector, I_E, was changed into a voltage signal, V_d, by a transimpedance amplifier (TIA), and read out by the lock-in amplifier. The measured admittance of silicon sub-bandgap photodetector can be expressed as

$$\tilde{Y} = I_E/V(f) = \left(V_d/G\right)/V(f) = Ye^{j\theta},$$

where G is the gain of TIA, $j=\sqrt{-1}$, θ is the phase. In all measurements thereafter, the amplitude of the driven voltage is 1 V, and $G = 10^7$ Ω. To make comparisons, five cases, without helium-ion implantation, with implanting doses of 1×10^{13}, 5×10^{13}, 1×10^{14}, and 1×10^{15} ions/cm^2, were investigated.

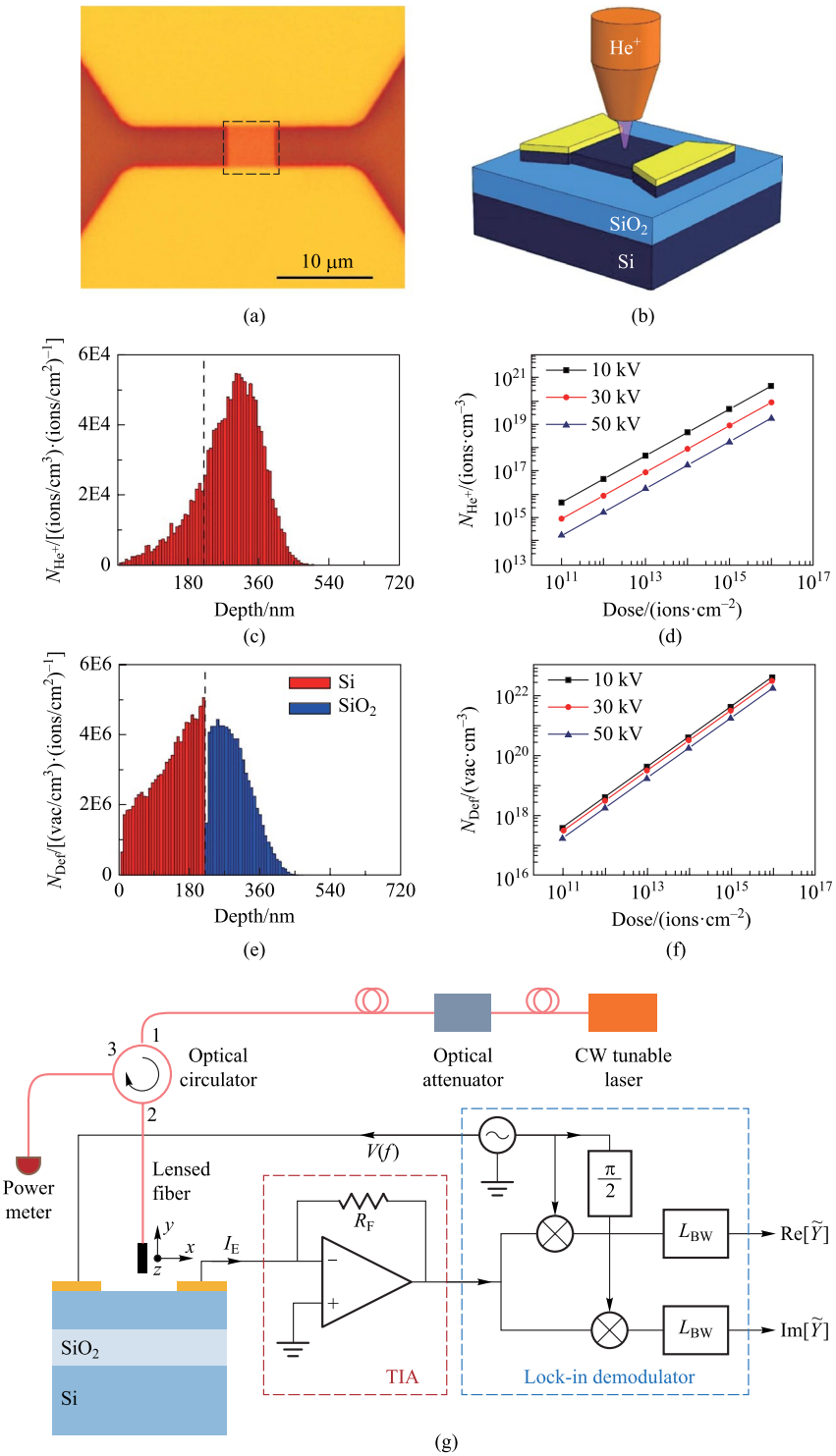

Fig. 1 Helium-ion implantation and device-testing setup. **a** Optical micrograph of the silicon sub-bandgap photodetector. The dashed box shows the area with helium-ion implantation. The area was 6.5 μm by 6.5 μm, slightly larger than the photosensitive area, 5 μm by 5 μm, of the photodetector. **b** Schematic drawing of locally implanting helium ions to the silicon sub-bandgap photodetector by using a helium-ion microscope. **c** Simulated helium-ion distribution per unit dose in the top silicon and silicon oxide. The accelerating voltage was 30 kV. **d** Monte–Carlo simulation of the volume density of the helium ions implanted in top silicon of the SOI wafer, as a function of the dose and at three accelerating voltage, 10, 30, and 50 kV. **e** Simulated defect distribution per unit dose in the top silicon and silicon oxide. The accelerating voltage was 30 kV. **f** Monte–Carlo simulation of the volume density of the vacancy generated in top silicon of the SOI wafer, as a function of the dose and at three accelerating voltages, 10, 30, and 50 kV. **g** Schematics of the experimental setup

3 Results and discussion

The first measurement was of the admittance in the dark, $Y(P=0)$. Figure 2 presents $Y(P=0)$ as a function of driven frequency, f. The results show that implantation did not affect $Y(P=0)$ except for very minor differences in the $Y-f$ curves. The interpretation was that the defect states generated by ion implantation made little contribution to the current transport when the photodetector was in the dark.

The second measurement was of the light-induced admittance variation, $\Delta Y(P) = |Y(P)| - |Y(P=0)|$, as a function of incident optical power, P. In this measurement, $f = 521$ Hz, and the lock-in bandwidth $\Delta f = 3$ Hz. Figure 3 presents the results and shows a dramatic enhancement of ΔY by helium-ion implantation. The error bar associated with each data point shows the standard deviation of 4499 measurements. For example, from Fig. 3, when the optical power is -10 dBm, ΔY of the sub-bandgap photodetector without helium ions implanted is 0.03 nS, ΔY of sub-bandgap photodetectors with an implantation dose of 1×10^{13}, 5×10^{13}, 1×10^{14}, and 1×10^{15} ions/cm^2 is 2.3, 3.0, 2.5 and 0.9 nS, respectively. The enhancement effect for the doses, 1×10^{13}, 5×10^{13} and 1×10^{14} ions/cm^2, is similar as indicated by the three almost identical curves of $\Delta Y(P)$. In particular, for the dose of 1×10^{13} ions/cm^2, the enhancement of the photo-response is 10log(2.3/0.03)=18.8 dB. We attribute this enhancement to the increase of the defect states within the bandgap, and therefore, the sub-bandgap optical absorption was enhanced. However, further increasing the implantation dose to 1×10^{15} ions/cm^2 weakened the enhancement effect.

The third measurement was the minimal detectable optical power, P_{sen}, at different lock-in bandwidth, Δf, as shown in Fig. 4. P_{sen} is defined by $\Delta Y(P_{sen}) = 6\sigma$, where σ is the standard deviation of $|Y(P=0)|$, representing the amplitude of the noise. P_{sen} characterizes the sensitivity of the sub-bandgap photodetector. In our experiment, σ stayed almost unchanged without and with helium-ion implantation. For the five cases investigated, the overall trend that P_{sen} increased as Δf increased was the same [5]. However, because helium-ion implantation enhanced the photo-response, as shown in Figs. 3 and 5, the photodetectors became more sensitive, i.e., P_{sen} decreased, compared with its value without helium-ion implantation. Specifically, when $\Delta f = 0.1$ Hz, P_{sen} of the silicon sub-bandgap photodetector without helium ions implanted was -33.2 dBm, and P_{sen} values of the silicon sub-bandgap photodetector implanted with helium ions at doses of 1×10^{13}, 5×10^{13}, 1×10^{14}, and 1×10^{15} ions/cm^2 were -63.1, -62.1, -61.2, and -49.2 dBm, respectively. The sensitivity was improved by 29.9, 28.9, 28, and 16 dB, respectively.

The fourth measurement was the spectral response. Two tunable semiconductor lasers were used, one ranging

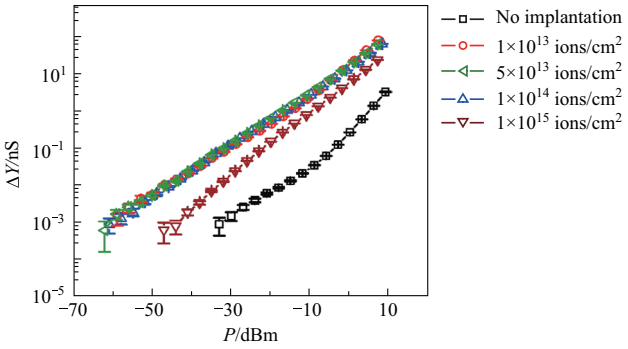

Fig. 3 Measured photo-response, ΔY, of the photodetector as a function of illuminating optical power, P. The driven frequency, f, was 521 Hz. Five cases were investigated: without helium-ion implantation, and with implanting doses of 1×10^{13}, 5×10^{13}, 1×10^{14}, and 1×10^{15} ions/cm^2

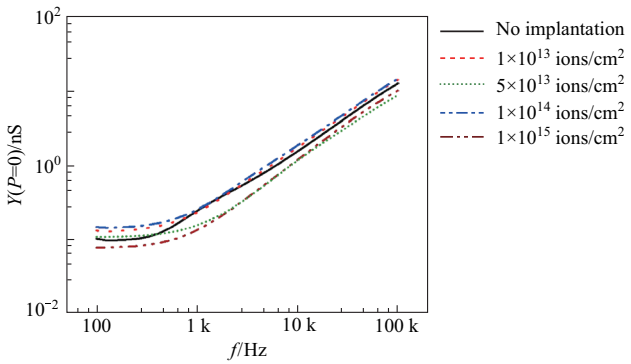

Fig. 2 Measured admittance, Y, of the photodetector as a function of driven frequency, f, without illumination. Five cases were investigated: without helium-ion implantation, and with implanting doses of 1×10^{13}, 5×10^{13}, 1×10^{14}, and 1×10^{15} ions/cm^2

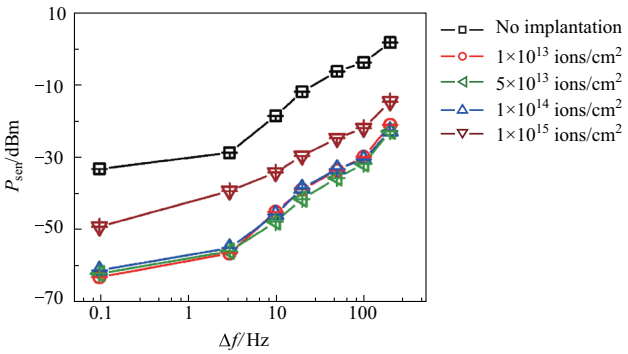

Fig. 4 Measured minimal detectable optical P_{sen} as a function of lock-in bandwidth, Δf. Five cases were investigated: without helium-ion implantation, and with implanting doses of 1×10^{13}, 5×10^{13}, 1×10^{14}, and 1×10^{15} ions/cm^2

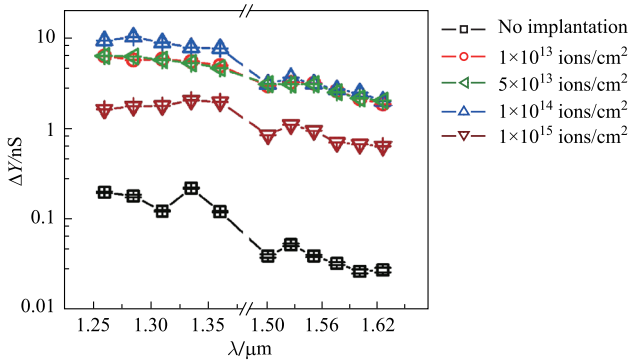

Fig. 5 Measured photo-response spectra of the photodetector. Five cases were investigated: without helium-ion implantation, and with implanting doses of 1×10^{13}, 5×10^{13}, 1×10^{14}, and 1×10^{15} ions/cm^2. The power of incident light was − 10 dBm

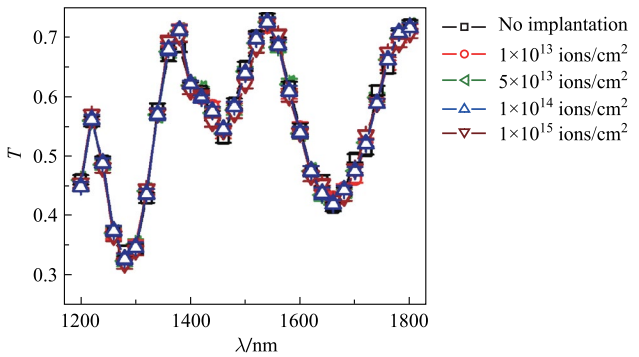

Fig. 6 Measured optical transmittance spectra of the photodetector. Five cases were investigated: without helium-ion implantation, and with implanting doses of 1×10^{13}, 5×10^{13}, 1×10^{14}, and 1×10^{15} ions/cm^2

from 1260 to 1360 nm and the other ranging from 1500 to 1630 nm. For these measurements, we kept the optical power to be − 10 dBm. As presented in Fig. 5, in these two bands, helium-ion implantation dramatically increased ΔY, showing this enhancement was broadband.

Finally, we measured the spectra (from 1200 to 1800 nm) of optical transmittance of the photosensitive region with and without helium implantation. To make these measurements, a SuperK with a monochromator was used as a tunable light source. A fiber focuser with an expanded mode field diameter of 4.3 μm was used to vertically illuminate a larger photosensitive region, 50 μm by 50 μm. The expansion of the mode size of the incident beam was necessary because otherwise the beam would have expanded too fast as it would have propagated such that the size of the beam would have been larger than the photosensitive region of the optical power meter used in our experimental setup. The optical transmittance was taken as $T = P_1/P_2$, where P_1 is the optical power transmitted through and P_2 is the incident power illuminating the silicon sub-bandgap photodetector. Each error bar in Fig. 6 represents the standard deviation of 50 measurements. The figure presents the results, showing that the spectra of the transmittance without helium-ion implantation and with implantation highly overlapped. The results mean that helium-ion implantation did not affect the transparency. We note in the figure that T maximizes at the wavelength of 1540 nm, and the maximum value of T is 73%. By appropriately coating anti-reflection coatings on the back of the photodetector, we can further increase T in this wavelength range.

We can now compare the advantages and disadvantages of helium ion implantation over other techniques to enhance the photodetection. Researchers enhance photodetection by optimizing the device structures and/or modifying the material properties. One example of a method for optimizing the device structures is to integrate the detectors with resonators [19]. This category of technique is typically used for enhancing the photodetection in a certain narrow band. In comparison, helium-ion implantation can enhance silicon sub-bandgap photodetection across a broad wavelength range, which is one advantage of this technique. On the other hand, use of the helium-ion microscope to implant the ions is a serial process and is only suitable for photodetectors with small photosensitive area. Moreover, the depth of implantation is limited, making this technique unsuitable for the cases that need to modify the material properties deeper in the photodetectors.

4 Conclusion

In conclusion, we have enhanced the photo-response of silicon sub-bandgap photodetectors by implanting helium ions with relatively low dose influences. With an implantation dose of 1×10^{13} ions/cm^2, the minimal detectable optical power was improved from − 33.2 to − 63.1 dBm, or, by 29.9 dB, at the wavelength of 1550 nm, and the photo-response at the same optical power (− 10 dBm) was enhanced by approximately 18.8 dB. We measured the transmittance spectra and observed no changes by helium-ion implantation. We attribute the enhancement of the photo-response to the increase of the defect states within the bandgap, which further increases the sub-bandgap optical absorption. This absorption, although being enhanced, still stays low ensuring the transparency of the photodetector. Our work provides a method for strategically modifying the intrinsic trade-off between transparency and strong photo-responses for this type of photodetectors.

Acknowledgements This work was supported by the National Key Research and Development Program of China (No. 2019YFB2203600)

and the Open Project Program of Wuhan National Laboratory for Optoelectronics (No. 2020WNLOKF003).

Author contributions ZW, KZ, HH, and XH designed the experiment. ZW and KZ fabricated the devices. XW and HH did the helium-ion implantation. ZW, KZ, and YM characterized the devices. ZW, KZ, JZ, JW, HH, XH analyzed the data. ZW and XH prepared the manuscript with the input and revisions from all authors. XH supervised the research. All authors read and approved the final manuscript.

Availability of data and materials The data that support the findings of this study are available from the corresponding author, upon reasonable request.

Declarations

Competing interests The authors declare that they have no competing interests.

References

1. Morichetti, F., Grillanda, S., Carminati, M., Ferrari, G., Sampietro, M., Strain, M.J., Sorel, M., Melloni, A.: Non-invasive on-chip light observation by contactless waveguide conductivity monitoring. IEEE J. Sel. Top. Quantum Electron. **20**(4), 292–301 (2014)
2. Grillanda, S., Carminati, M., Morichetti, F., Ciccarella, P., Annoni, A., Ferrari, G., Strain, M., Sorel, M., Sampietro, M., Melloni, A.: Noninvasive monitoring and control in silicon photonics using CMOS integrated electronics. Optica **1**(3), 129–136 (2014)
3. Grimaldi, V., Zanetto, F., Toso, F., Vita, C., Ferrari, G.: Noninvasive light sensor with enhanced sensitivity for photonic integrated circuits. In 17th conference on Ph.D. research in microelectronics and electronics (PRIME). IEEE, pp. 285–288 (2022)
4. Wang, Z., Zhang, Z., Zou, K., Meng, Y., Liu, H., Hu, X.: Noise properties of contactless integrated photonic probes on silicon waveguides. Appl. Opt. **62**(1), 178–182 (2023)
5. Wang, Z., Liu, H., Zhang, Z., Zou, K., Hu, X.: Infrared photoconductor based on surface-state absorption in silicon. Opt. Lett. **46**(11), 2577–2580 (2021)
6. Zhang, Z., Wang, Z., Zou, K., Yang, T., Hu, X.: Temperature-dependent characteristics of infrared photodetectors based on surface-state absorption in silicon. Appl. Opt. **60**(30), 9347–9351 (2021)
7. Wang, Z., Zhang, Z., Zou, K., Meng, Y., Hu, X.: Silicon four-quadrant photodetector working at the 1550-nm telecommunication wavelength. Opt. Lett. **47**(16), 4048–4051 (2022)
8. Allen, F.I.: A review of defect engineering, ion implantation, and nanofabrication using the helium ion microscope. Beilstein J. Nanotechnol. **12**(1), 633–664 (2021)
9. Wen, X., Mao, R., Hu, H.: 3-D nanofabrication of silicon and nanostructure fine-tuning via helium ion implantation. Adv. Mater. Interfaces **9**(10), 2101643 (2022)
10. Liu, Y., Chow, C.W., Cheung, W.Y., Tsang, H.K.: In-line channel power monitor based on helium ion implantation in silicon-on-insulator waveguides. IEEE Photon. Technol. Lett. **18**(17), 1882–1884 (2006)
11. Wang, B., Zhang, Y., Tang, L., Deng, G., Teng, K., Wu, G., Song, L.: Silicon based mesa heterojunction photodetector. Earth and Space: From Infrared to Terahertz (ESIT 2022). SPIE **12505**, 71–75 (2023)
12. Zheng, X., Ma, S., Zhang, Y., Wang, M., Fan, H., Feng, H.: Enhancement of $CsPbBr_3$ perovskite single-crystal photodetector performance via Zr ion implantation. J. Phys. Chem. C **127**, 11780–11786 (2023)
13. Wang, Z., Yuan, L., Wang, Y., Wang, J., Zhang, Y., Jia, R.: Mg ion implantation and post-annealing effect on the photoelectrical performance of a β-Ga_2O_3 photodetector. Appl. Opt. **62**(15), 3848–3854 (2023)
14. Li, C., Zhao, J., Liu, X., Ren, Z., Yang, Y., Chen, Z., Chen, Q., Sun, H.: Record-breaking-high-responsivity silicon photodetector at infrared 1.31 and 1.55 μm by argon doping technique. IEEE Trans. Electron Devices **70**(5), 2364–2369 (2023)
15. Bornacelli, J., Araiza-Sixtos, F., Torres-Torres, C., Hernández-Acosta, M., Oliver, A., Angel-Rojo, R.: Driving third-order optical nonlinearities in photoluminescent si nanoparticles by nitrogen co-implantation in a silica matrix. Materials **15**(16), 5670 (2022)
16. Cho, E., Zhou, Y., Cho, J., Cybart, S.: Superconducting nano Josephson junctions patterned with a focused helium ion beam. Appl. Phys. Let. **113**(2), 022604 (2018)
17. Jadwiszczak, J., Keane, D., Maguire, P., Cullen, C., Zhou, Y., Song, H., Downing, C., Fox, D., McEvoy, N., Zhu, R., Xu, J., Duesberg, G., Liao, Z., Boland, J., Zhang, H.: MoS_2 memtransistors fabricated by localized helium ion beam irradiation. ACS Nano **13**(12), 14262–14273 (2019)
18. Ziegler, J., Biersack, J., Littmark, U.: The Stopping and Range of Ions in Solids. Pergamon, New York, (1985). See www.srim.org/ for SRIM version, 2013.
19. Chen, H., Luo, X., Poon, A.: Cavity-enhanced photocurrent generation by 1.55 μm wavelengths linear absorption in a p-i-n diode embedded silicon microring resonator. Appl. Phys. Lett. **95**(17), 171111 (2009)

Zhao Wang received his B. S. degree in Optoelectronics Information Science and Engineering from Changchun University of Science and Technology, China in 2018. He is now a Ph.D. candidate majoring in Optical Engineering at Tianjin University, China. His current research focuses on silicon-photonic devices.

Xiaolei Wen is a senior engineer at Center for Micro and Nanoscale Research and Fabrication at University of Science and Technology of China (USTC), China. She obtained her Ph.D. degree from the Department of Optics and Optical Engineering at USTC and has completed two years of joint training in the Department of Mechanical Engineering at Purdue University, USA. Her current research focuses on advanced micro/nano fabrication and characterization technologies, particularly novel fabrication techniques for silicon and third-generation semiconductor material using helium-ion microscopy.

Kai Zou received his B. S. degree in Optical Engineering from Tianjin University, China in 2019. He is now a Ph.D. candidate majoring in Optical Engineering at Tianjin University. His current research focuses on superconducting nanowire single-photon detectors (SNSPDs) and silicon-photonic devices.

Yun Meng received his B.S. degree in Applied Physics from Southwest Jiaotong University, China in 2018. He is now a Ph.D. candidate majoring in Optical Engineering at Tianjin University, China. His current research focuses on superconducting nanowire single-photon detectors (SNSPDs) and silicon-photonic devices.

Jinwei Zeng received the Ph.D. degree in Electric Engineering from the State University of New York at Buffalo, USA in 2014. He worked as Postdoc Scholar in Missouri University of Science and Technology, USA from 2015 – 2016, and in University of California Irvine, USA from 2016 – 2018. He joined Huazhong University of Science and Technology, China as a faculty member from 2019 till present. He is currently an Associate Professor in Wuhan National Laboratory for Optoelectronics, Huazhong University of Science and Technology, China. He has served as the secretary of IEEE Optical Society Wuhan Chapter since 2020. His research interest is mainly in the sciences and applications of Nanophotonics, including metamaterials/metasurfaces, structured light, photo-induced force microscopy, optical magnetism etc.

Jian Wang received the Ph.D. degree in Physical Electronics from the Wuhan National Laboratory for Optoelectronics, Huazhong University of Science and Technology, China in 2008. He worked as a Postdoctoral Research Associate in the Optical Communications Laboratory, University of Southern California, USA from 2009 to 2011. He is currently a professor at the Wuhan National Laboratory for Optoelectronics, Huazhong University of Science and Technology, China. He is the vice director of Wuhan National Laboratory for Optoelectronics, Huazhong University of Science and Technology, China. He leads the Multi-Dimensional Photonics Laboratory (MDPL). His research interests include optical communications, optical signal processing, silicon photonics, photonic integration, orbital angular momentum, and structured light. He has published over 260 refereed international journal papers on *ScienceScience AdvancesNature PhotonicsNature CommunicationsLight: Science & ApplicationsPhysical Review LettersOpticaLaser & Photonics ReviewsResearchPhotoniXAdvanced PhotonicsACS Photonics*, etc. He has authored and co-authored over 150 international conference papers on OFC, ECOC, CLEO, etc. He has also given over 110 tutorial/keynote/invited talks in international conferences including the invited talk at OFC2014 and tutorial talk at OFC2016. He is currently an OPTICA Fellow and an SPIE Fellow. He is also an Executive Editor-in-Chief of *Frontiers of Optoelectronics*, Topical Editor of *Optics Letters*, Deputy Editor of *Chinese Optics Letters*, and Area Editor of *Microwave and Optical Technology Letters*. He is also a frequent reviewer of *Nature Photonics* and *Nature Communications*.

Huan Hu is a tenure-track assistant professor at ZJU-UIUC Institute at the international campus of Zhejiang University, China. he is an associate editor in *Frontiers in Sensors*, an ad-hoc member in *IEEE TED*, a council member of MEMS & NEMS Society of China. He received the B.S and M.S degrees from Tsinghua University, China and Ph.D. degree from University of Illinois at Urbana-Champaign (UIUC), USA in Electrical and Computer Engineering. He did his postdoc training in IBM T. J. Watson Research Center, USA. He focuses on advanced nanofabrication and measurement and highly engages in interdisciplinary research. He has published more than 71 peer-reviewed papers on 42 different journals covering electronics, mechanics, biomedicine, chemistry, and materials. He has filed 28 U.S patents (18 granted) and 10 C.N. patents (4 granted).

Xiaolong Hu is a professor with the School of Precision Instruments and Optoelectronic Engineering at Tianjin University, China, where he heads the Nanophotonics Group. He obtained his Ph.D. degree from the Department of Electrical Engineering and Computer Science at the Massachusetts Institute of Technology, USA in 2011. He is a senior member of IEEE, Optica (formerly OSA), the Chinese Optical Society, and SPIE. He is now serving as an associate editor of *Optics Continuum*, an associate editor of *Frontiers in Photonics* (Quantum Optics specialty section), an early-career editorial board member of *Frontiers of Optoelectronics*, and an editorial board member of *Scientific Reports*. His current research interests include nanophotonic devices, quantum photonics, and LiDAR.